The EMBO Journal Vol.16 No.13 pp.4049–4059, 1997

Formation of plant RNA virus replication complexes on membranes: role of an endoplasmic reticulum-targeted viral protein

Mary C.Schaad[1], Patricia E.Jensen and James C.Carrington[1,2]

Department of Biology, Texas A & M University, College Station, TX 77843, USA

[1]Present address: Institute of Biological Chemistry, Clark Hall, Washington State University, Pullman, WA 99164-6340, USA

[2]Corresponding author

The mechanisms that direct positive-stranded RNA virus replication complexes to plant and animal cellular membranes are poorly understood. We describe a specific interaction between a replication protein of an RNA plant virus and membranes *in vitro* and in live cells. The tobacco etch virus (TEV) 6 kDa protein associated with membranes as an integral protein via a central 19 amino acid hydrophobic domain. In the presence or absence of other viral proteins, fluorescent fusion proteins containing the 6 kDa protein associated with large vesicular compartments derived from the endoplasmic reticulum (ER). Infection by TEV was associated with a collapse of the ER network into a series of discrete aggregated structures. Viral RNA replication complexes from infected cells were also associated with ER-like membranes. Targeting of TEV RNA replication complexes to membranous sites of replication is proposed to involve post-translational interactions between the 6 kDa protein and the ER.

Keywords: endoplasmic reticulum/replication complex/ RNA virus/tobacco etch virus

Introduction

The genomes of positive-strand RNA viruses replicate in close association with membranes (see reviews by Wimmer *et al*., 1993; Strauss and Strauss, 1994). In fact, some viruses have been shown to induce proliferation or reorganization of cellular membranes and vesicles, possibly as a mechanism to increase the available surface area for RNA synthesis. In the case of picornaviruses, for example, RNA replication complexes are associated with clusters of smooth vesicles that accumulate in the cytoplasm (Bienz *et al*., 1983, 1987, 1992; Troxler *et al*., 1992). The mechanisms whereby replication complexes are fixed to specific types of membranes are poorly understood, although the involvement of viral proteins as membrane anchors has been proposed (see reviews by Semler *et al*., 1988; Wimmer *et al*., 1993). Understanding the ways in which viral proteins and replication complexes interact with membranes will shed considerable light on the critical virus–cell interactions that facilitate infection of plants and animals.

Tobacco etch potyvirus (TEV) is a well-characterized member of the 'picornavirus supergroup' of positive-strand RNA viruses (Koonin and Dolja, 1993). The TEV–plant model system has been extremely useful for analysis of viral replication and intercellular movement, partly because of the ease with which the viral and plant genomes can be modified (Dolja *et al*., 1992, 1994; Restrepo-Hartwig and Carrington, 1994; Li and Carrington, 1995). All TEV-encoded proteins arise by synthesis of a large polyprotein followed by co- and post-translational processing catalyzed by three proteinases (Dougherty and Semler, 1993) (Figure 1). Several TEV proteins, including CI, 6 kDa protein, NIa and NIb, are required for genome replication (Klein *et al*., 1994; Restrepo-Hartwig and Carrington, 1994; Li and Carrington, 1995; Murphy *et al*., 1996; Schaad *et al*., 1996), most likely as core components of a replication complex. The CI protein contains an ATP-dependent RNA-unwinding activity and amino acid sequence similarity with known helicases (Laín *et al*., 1990, 1991). The multifunctional NIa protein contains two discrete domains: the N-terminal VPg domain that attaches covalently to the 5′ terminus of viral RNA (Shahabuddin *et al*., 1988; Murphy *et al*., 1990b) and a C-terminal picornavirus 3C-like proteinase domain (Carrington and Dougherty, 1987b; Hellmann *et al*., 1988; García *et al*., 1989). Most of the polyprotein cleavages are catalyzed by the NIa proteinase. The NIb protein, which interacts specifically with NIa in the yeast two-hybrid system (Hong *et al*., 1995; Li *et al*., 1997), is the probable catalytic subunit of the viral RNA-dependent RNA polymerase (Allison *et al*., 1986; Domier *et al*., 1987). The 6 kDa protein has no known enzymatic functions, but immunocytochemical and biochemical evidence indicates that it associates closely with membranes (Restrepo-Hartwig and Carrington, 1994).

Despite their requirement in the cytoplasm or in membrane-bound replication complexes, both NIa and NIb accumulate predominantly in the nucleus of TEV-infected cells (Baunoch *et al*., 1988; Restrepo *et al*., 1990). Their function in the nucleus is not known. However, a subset of NIa was postulated to be directed toward membranes in a polyprotein form containing the 6 kDa protein (Restrepo-Hartwig and Carrington, 1994). When present within the same polyprotein, the membrane-binding activity of the 6 kDa protein dominates over the nuclear localization activity of NIa (Restrepo-Hartwig and Carrington, 1992). Direction of the VPg towards membranes through covalent association with a membrane-binding protein may be a highly conserved feature among the picornavirus supergroup members (Wimmer *et al*., 1993). The TEV 6 kDa protein, therefore, is proposed to function as an anchor to secure part or all of the TEV RNA replication apparatus to membranous sites.

In this study, the nature of the interaction between the 6 kDa protein and membranes was explored. Using a

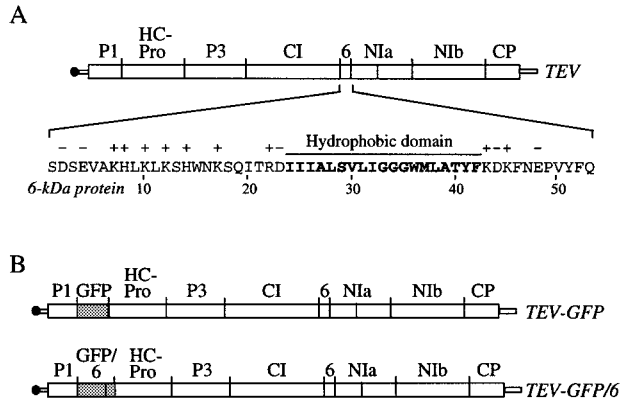

Fig. 1. Diagrammatic representation of the TEV, TEV-GFP and TEV-GFP/6 genomes. (**A**) Schematic diagram of the TEV genome and amino acid sequence of the 6 kDa protein. The map is drawn to scale with the individual coding regions indicated above the diagram. Sequences coding for proteolytic cleavage sites are indicated by vertical lines. The VPg at the 5′ terminus is represented as a filled circle. The sequence of the 6 kDa protein is drawn with the central hydrophobic domain in bold and charged residues indicated. (**B**) Schematic diagrams of the TEV-GFP and TEV-GFP/6 genomes. The GFP- or GFP/6-coding sequences between the P1- and HC-Pro-coding regions are shaded.

variety of transient and virus vector-based expression systems involving fusions between the 6 kDa protein and reporter proteins, the specific membranes interacting with the 6 kDa protein were identified and visualized in live cells. In addition, membranes containing TEV plus-strand RNA synthesis activity were shown to have properties similar to those that associated with the 6 kDa protein.

Results

The TEV 6 kDa protein is an integral membrane protein

To determine whether the TEV 6 kDa protein is an integral or peripheral membrane protein, biochemical analyses were performed using fractions isolated from transgenic plants expressing β-glucuronidase (GUS) or a fusion protein containing GUS and the 6 kDa protein (GUS/6). The GUS/6 fusion protein was shown previously, using fractionation and immunolocalization methods, to associate with membranes (Restrepo-Hartwig and Carrington, 1994). The GUS protein was detected primarily in the soluble S30 fraction (Figure 2, lanes 1 and 2), whereas the GUS/6 fusion protein was predominantly in the P30 crude membrane fraction (lanes 3 and 4). The GUS/6 protein remained associated with the membrane fraction after extraction with 1 M KCl, 4 M urea or 0.1 M Na_2CO_3, pH 10.5 (Figure 2, lanes 5–10). These treatments would be expected to dislodge proteins that were weakly or peripherally associated with membranes. A Triton X-114 phase partition analysis was also done. In this experiment, the P30 fraction (Figure 2, lane 11) contained both full-length GUS/6 fusion protein and an apparent breakdown product. The GUS/6 fusion protein, but not the breakdown product, partitioned mainly to the detergent phase (Figure 2, lanes 12 and 13.) The behavior of the GUS/6 fusion protein during these treatments strongly suggests that the 6 kDa protein associates with membranes as an integral protein.

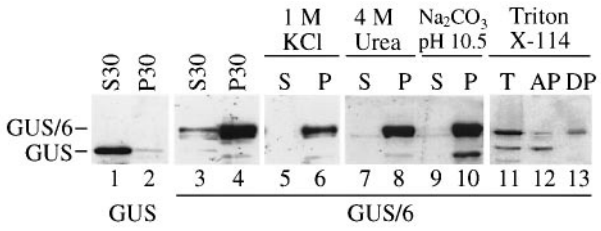

Fig. 2. Extraction and immunoblot analysis of GUS and GUS/6 fusion protein expressed in transgenic tobacco plants. Total S30 and P30 fractions from GUS- (lanes 1 and 2) and GUS/6- (lanes 3 and 4) expressing transgenic plants were analyzed. The P30 fraction from GUS/6 plants was extracted with 1 M KCl, 4 M urea or 0.1 M Na_2CO_3 (pH 10.5) and subjected to centrifugation at 30 000 *g*, yielding S30 (S) and P30 (P) fractions (lanes 5–10). The total (T) P30 fraction was also fractionated into aqueous (AP) and detergent-soluble (DP) phases after treatment with Triton X-114 (lanes 11–13).

6 kDa protein associates with vesicular membranes

To visualize and characterize the TEV 6 kDa protein–membrane interaction in live cells, transient expression vectors encoding non-fused green fluorescent protein (GFP) or a fusion protein containing GFP and the 6 kDa protein were constructed (Figure 3). These plasmids were introduced into tobacco leaf epidermal cells by biolistic delivery, and GFP or GFP/6 were detected by fluorescence microscopy. Cells containing non-fused GFP contained fluorescence throughout the cytoplasm and in or around the nucleus (Figure 4A). Cells with GFP/6 contained fluorescence in discrete, vesicular compartments (Figure 4B and C). Higher magnification clearly revealed that the compartments were fluorescent at their periphery rather than their interior (Figure 4D). The vesicles often, but not always, accumulated around the nucleus; in fact, the periphery of the nucleus frequently contained GFP fluorescence (Figure 4D). The vesicles were 2–10 μm in diameter, and were often observed to be motile.

To verify that the vesicular localization pattern was not an artifact of the biolistic delivery method, and to determine the effect of virus infection on 6 kDa protein-mediated localization to vesicles, GFP and GFP/6 were expressed from engineered TEV vectors (Figure 1B). TEV-GFP and TEV-GFP/6 were indistinguishable with regard to rate of systemic movement and induction of symptoms. Protoplasts from non-infected or systemically infected leaves were examined by fluorescence microscopy. Non-infected protoplasts contained no fluorescence (Figure 5A), whereas TEV-GFP-infected protoplasts contained GFP fluorescence throughout the cytoplasm and in or around the nucleus (Figure 5B). Protoplasts from TEV-GFP/6-infected plants contained fluorescence localized to vesicles that were similar to those visualized in the bombarded epidermal cells (Figure 5C–E). In some cases, the vesicles were distended or clustered near the nucleus. This indicates that the 6 kDa protein, in the presence or absence of TEV infection, mediates an association with vesicular membranes.

Vesicle association requires a central hydrophobic domain in the 6 kDa protein

A series of deletions was introduced into the 6 kDa protein-coding region in the transient expression vector encoding GFP/6 (Figure 3), and the modified constructs

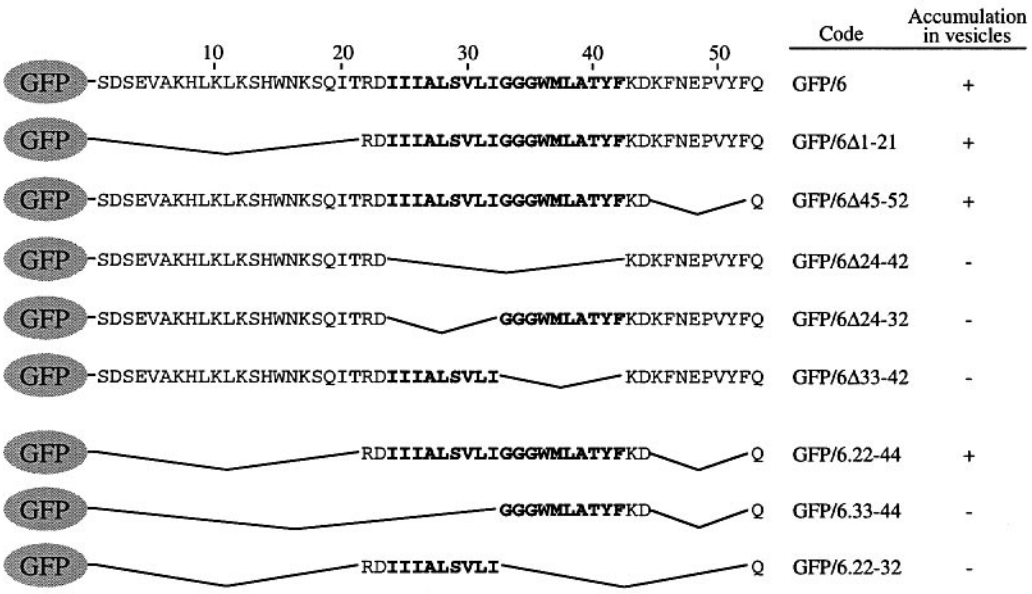

Fig. 3. Diagrammatic representation of the GFP/6 fusion proteins expressed in tobacco epidermal cells. Expression plasmids encoding fusion proteins were introduced into epidermal cells of tobacco leaves by biolistic delivery. The accumulation of GFP fluorescence in association with vesicles (+) or distributed throughout the cytosol and nucleus (–) was scored by fluorescence microscopy. The central hydrophobic region of the 6 kDa protein is indicated by bold type.

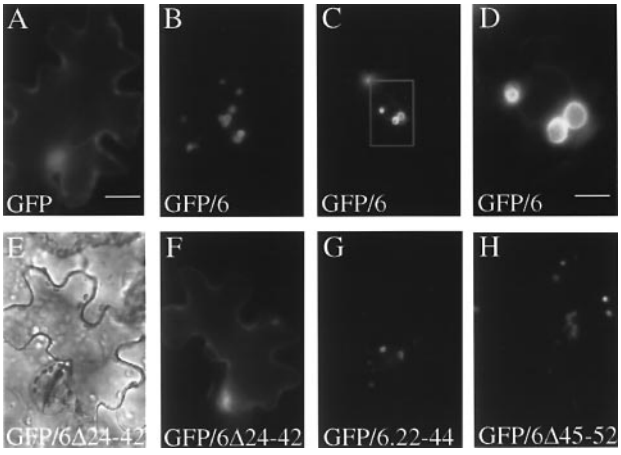

Fig. 4. Transient expression and visualization of GFP and GFP/6 fusion proteins in tobacco epidermal cells. Cells were bombarded with expression plasmids encoding the proteins indicated in each panel and examined by fluorescence (**A**–**D** and **F**–**H**) or brightfield (**E**) microscopy at 16 h post-bombardment. Brightfield and fluorescence micrographs for the same field of view are shown in (E) and (F). All micrographs are shown at the same magnification, except in (D), which is an enlargement of the boxed area in (C). Bars equal 29 μm (A) and 10 μm (D).

were introduced by biolistic delivery into tobacco epidermal cells. The deletions affected the hydrophilic N-terminal region (residues 1–21), the central hydrophobic domain (residues 24–42) or the C-terminal region (residues 45–52). Deletion variants lacking either the N-terminal 21 residues (GFP/6Δ1–21) or eight of nine C-terminal residues (GFP/6Δ45–52) were able to associate with vesicles (Figures 3 and 4A and H, and data not shown). In contrast, deletion variants lacking the central 19 residues comprising the hydrophobic domain (GFP/6Δ24–42), or lacking the first or second halves of the hydrophobic domain (GFP/6Δ24–32 and GFP/6Δ33–42), accumulated throughout the bombarded cell cytoplasm and nucleus in a manner similar to non-fused GFP (Figures 3 and 4F, and data not shown). A double deletion variant containing GFP fused to residues 22–44 (GFP/6.22–44), which comprises the hydrophobic domain plus two charged residues on either side, associated with vesicles (Figures 3 and 4G). Double deletion variants lacking either half of the hydrophobic domain (GFP/6.33–44 and GFP/6.22–32) accumulated throughout the cytoplasm (Figure 3 and data not shown). These results indicate that the central hydrophobic domain, but not the N- or C-terminal regions, is necessary for vesicle association.

6 kDa protein mediates association with endoplasmic reticulum-derived membranes

Immunofluorescence using antibodies specific for proteins of the endoplasmic reticulum (ER) (BiP) or the *medial*- and *trans*-Golgi (proteins containing xylose β,1→2 mannose modifications) was carried out with TEV-GFP/6-infected protoplasts. In preliminary experiments, GFP fluorescence was preserved after fixation in buffered 4% paraformaldehyde followed by brief 95% ethanol treatments, but not after fixation in 50% ethanol/4% paraformaldehyde/5% acetic acid; protoplasts were fixed, therefore, using the former protocol (Chalfie *et al*., 1994). Selection of Cy3 as the secondary antibody permitted dual localization of GFP/6 and the respective marker proteins using two filter sets during fluorescence microscopy. Although the protoplasts often lost their regular round appearance after fixation and subsequent incubations, GFP/6-containing vesicles or membrane aggregates were clearly visible (Figure 6).

In protoplasts treated with anti-BiP serum, GFP/6 was detected in structures that also contained BiP, although BiP was always present in additional structures throughout the cell (Figure 6A). GFP/6-labeled vesicles co-localized strongly with BiP in 87.5% of cells ($n = 64$) that contained both GFP/6 fluorescence and anti-BiP immunofluores-

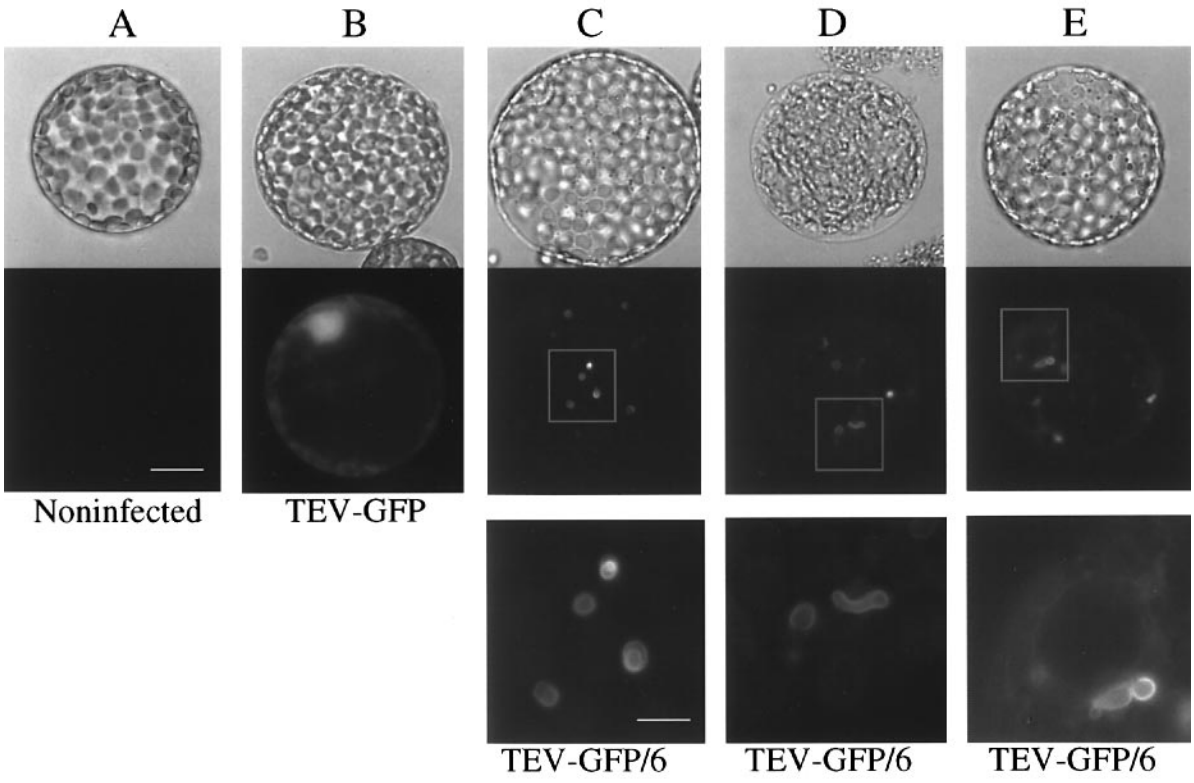

Fig. 5. Expression and visualization of GFP and GFP/6 using recombinant TEV vectors in live protoplasts from infected tobacco plants. Micrographs in each vertical series shows brightfield (top) and fluorescence (middle and bottom) images from the same non-infected (**A**), TEV-GFP-infected (**B**) or TEV-GFP/6-infected (**C**–**E**) protoplast. The top and middle rows of micrographs are shown at the same magnification; the fluorescence micrographs at the bottom are enlargements of the boxed areas. Bars equal 46 μm (A) and 15 μm (C, bottom).

cence. In some cells, however, GFP/6-containing structures that lacked detectable BiP were also detected (Figure 6A). Vesicles containing GFP/6 co-localized strongly with β-xylosyl-containing proteins in only 9.2% of cells (n = 87); the remaining cells (90.8%) contained little or no detectable co-localization (Figure 6B). Protoplasts treated with Cy3-labeled secondary antibody but no primary antibody exhibited GFP/6 fluorescence but no Cy3 fluorescence (Figure 6C). These results suggest that a high proportion of GFP/6-containing vesicles contain protein associated with the ER.

To characterize further the membranes to which the 6 kDa protein attaches, sucrose gradients were used to resolve membranes recovered from TEV-GFP- and TEV-GFP/6-infected tissue. Membranes from half-leaves were extracted and analyzed on sucrose gradients under high (3 mM) or low (0.1 mM) $MgCl_2$ conditions. Sucrose gradient fractions were analyzed by immunoblot assay using anti-GFP, anti-BiP and anti-β-xylosyl sera. The specificity of anti-GFP serum was tested in preliminary experiments using total SDS-soluble protein extracts and sucrose gradient fractions from non-infected plants, and using total proteins from TEV-GFP-infected and TEV-GFP/6-infected plants. No reactivity was detected in total extracts or in any sucrose gradient fraction recovered from non-infected plants (Figure 7A). Single proteins of the sizes predicted for GFP and GFP/6 were detected in total extracts from TEV-GFP- and TEV-GFP/6-infected plants, respectively (Figure 7A; molecular mass markers not shown). In preliminary experiments with anti-BiP and anti-β-xylosyl sera using total extracts, anti-BiP serum reacted with a single protein of ~70 kDa, as anticipated, whereas the anti-β-xylosyl serum reacted with numerous proteins (data not shown). Reaction of anti-β-xylosyl serum with numerous proteins was expected, as this antiserum recognizes a carbohydrate moiety added to proteins traversing, or residing within, the Golgi apparatus (Laurière *et al*., 1989; Zhang and Staehlin, 1992).

The first series of gradients were carried out in the presence of 3 mM $MgCl_2$, which preserves the integrity of ribosomes associated with rough ER (RER) (Lord *et al*., 1973; Wienecke *et al*., 1982). Non-fused GFP from TEV-GFP-infected tissue remained at the top of the sucrose gradient (Figure 7B), which is consistent with its localization in the cytosol. The GFP/6 fusion protein from TEV-GFP/6-infected tissue, however, sedimented to a position near the bottom of the gradient (Figure 7C; peak fractions 6–7). The same gradient fractions were assayed for BiP and β-xylosyl-containing proteins. Two BiP-containing peaks were resolved, one near the top and one near the bottom of the gradient (Figure 7D), the latter of which was coincident with the GFP/6-containing peak. The heavy BiP-containing fractions contained rRNA (data not shown) and were present in the gradient at positions consistent with previous analyses of ER from plants (Wienecke *et al*., 1982). The heavy peak, therefore, was concluded to contain ER membranes, with at least some of the membrane associated with ribosomes. The nature of the light BiP-containing peak was not determined. The constellation of β-xylosyl-containing proteins was detected near the top of the gradient (Figure 7E).

The second series of gradients were done simultaneously

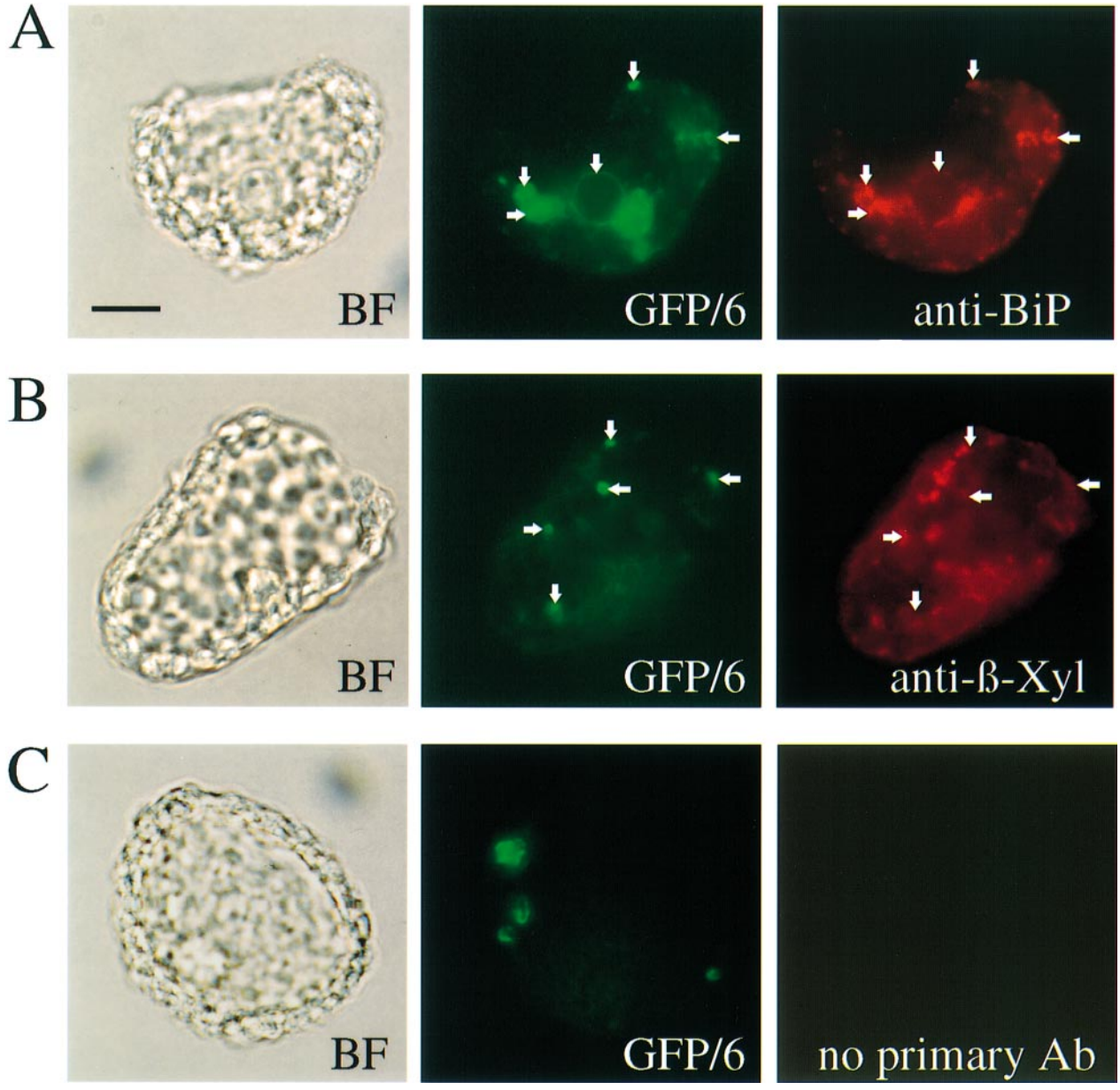

Fig. 6. Immunofluorescence localization of BiP and β-xylosyl-containing proteins in TEV-GFP/6-infected protoplasts. Micrographs in each horizontal row show brightfield (BF, left), GFP/6 fluorescence (middle) and Cy3 secondary antibody fluorescence (right) images from the same protoplast. Primary antibody was anti-BiP (**A**) or anti-β-xylosyl (**B**). No primary antibody was used in (**C**). All micrographs are shown at the same magnification. The arrows in (A) and (B) are placed at identical positions within the complementary photomicrographs of each cell. Bar in (A) equals 35 μm.

with the 3 mM $MgCl_2$ gradients but in the presence of 0.1 mM $MgCl_2$. The low $MgCl_2$ concentration promotes destabilization of RER-associated ribosomes, resulting in a shift of the heavy ER to lighter fractions of the gradient (Wienecke *et al*., 1982). The GFP/6 peak was shifted up the gradient by ~3–4 fractions under the low $MgCl_2$ conditions (Figure 7C). The heavy BiP peak was also shifted up the gradient in low $MgCl_2$ conditions to an extent similar to the GFP/6 shift, resulting in an overlap with the light BiP fractions (Figure 7D). A similar $MgCl_2$-dependent shift was detected using antiserum against protein disulfide isomerase, another ER luminal protein (data not shown). No effect of $MgCl_2$ was detected on the distribution of β-xylosyl-containing proteins (Figure 7E). The immunofluorescence and membrane fractionation data strongly suggest that the GFP/6-containing membrane shares properties in common with the ER.

Infection by TEV alters the morphology of the endoplasmic reticulum

To determine whether or not the morphology of the ER is affected by TEV infection, the organization of the ER in TEV-infected and non-infected cells was compared. Transgenic *Nicotiana benthamiana* plants expressing an ER-targeted GFP (mGFP5) were used. Epidermal cells were obtained from non-infected or systemically infected leaves and observed by fluorescence microscopy. In non-infected cells, the ER was characterized by an extensive, interconnected network of tubules that was distributed uniformly throughout the cytoplasm (Figure 8A). In many

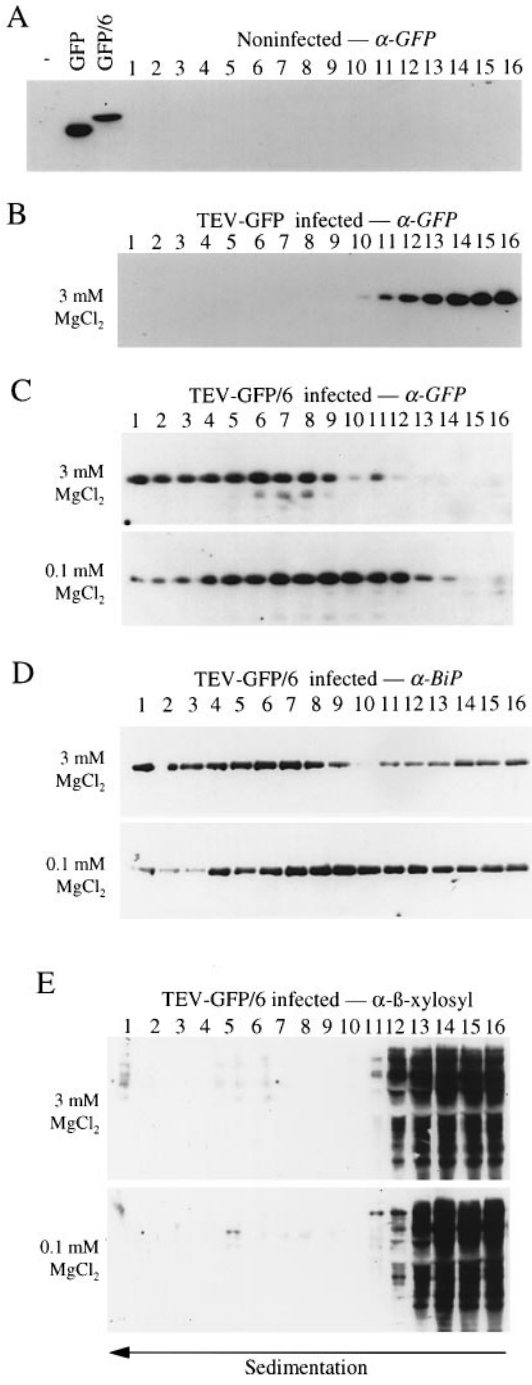

Fig. 7. Sucrose gradient analysis of membranes with GFP/6, BiP and β-xylosyl-containing proteins. Tissue extracts were prepared and fractionated on 20–45% sucrose density gradients in the presence of either 0.1 mM $MgCl_2$ or 3 mM $MgCl_2$. The direction of sedimentation was from right to left, with fraction 16 representing the top of each gradient. (**A**) Sucrose gradient using non-infected extracts and immunoblot analysis using anti-GFP serum. Non-fractionated extracts were also analyzed from non-infected (–), TEV-GFP-infected (GFP) or TEV-GFP/6-infected (GFP/6) plants. (**B**) Sucrose gradient using TEV-GFP-infected extracts and immunoblot analysis using anti-GFP serum. (C–E) Sucrose gradients using TEV-GFP/6-infected extracts and immunoblot analysis using anti-GFP (**C**), anti-BiP (**D**) and anti-β-xylosyl (**E**). In (E), only β-xylosyl-containing proteins with apparent mol. wts between 25 and 70 kDa are shown.

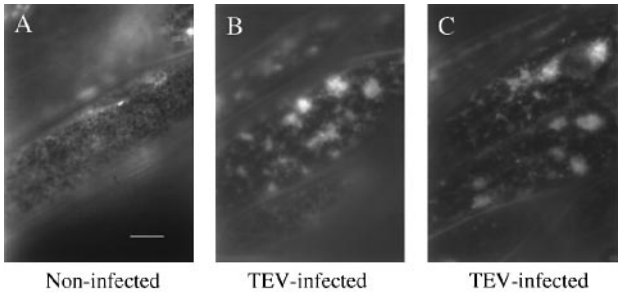

Fig. 8. Visualization of the ER in infected and non-infected cells. The ER was visualized in live epidermal cells of transgenic *N.benthamiana* plants expressing an ER-targeted form of GFP by fluorescence microscopy. All micrographs are shown at the same magnification. Bar in (A) equals 20 μm. (**A**) An epidermal cell in a leaf of a non-infected plant. (**B** and **C**) Epidermal cells in upper, systemically infected leaves at 6 days post-inoculation.

cells, fluorescence was associated with streaming structures. Fluorescent vesicles of <1 μm in diameter were often associated with the network. The periphery of the nucleus, but not the nucleoplasm, was consistently fluorescent. Similar observations were made using an ER-targeted GFP expressed from a recombinant potato virus X vector (Boevink *et al*., 1996).

The ER in TEV-infected cells differed dramatically from the ER in non-infected cells. Infected epidermal cells from upper leaves were identified based on the presence of TEV-induced nuclear inclusion bodies, which were clearly visible using differential interference contrast microscopy (data not shown). Fluorescence was not associated with a uniform network, but rather was concentrated in amorphous aggregates that appeared to be compacted ER (Figure 8B and C). In most instances, the aggregates were linked by a limited number of ER-like tubules (Figure 8C). This pattern of fluorescence was observed consistently in five separate experiments, in which ~10 strips of epidermal cells from each of several infected plants were examined exhaustively. In no instance was ER aggregation detected in cells from non-infected plants, or in cells that lacked evidence of TEV infection (i.e. nuclear inclusion bodies) from inoculated plants, implying strongly that the morphological changes of the ER were a consequence of TEV infection.

Viral RNA synthesis activity co-fractionates with the ER

Membrane-bound RNA-dependent RNA polymerase (RdRp) associated with endogenous template was isolated from TEV-infected tissue and subjected to sucrose gradient analysis. In initial experiments, [^{32}P]UTP-labeled RNA products synthesized in a washed P30 fraction (P30-2) from TEV-infected and non-infected tissue were characterized. Two RNA species were synthesized using the extracts from infected tissue—one migrated to a position corresponding to TEV genomic RNA and the other migrated as a broad band to a position slightly above that of synthetic TEV double-stranded RNA (Figure 9A, lane 1). The faster migrating product was susceptible to RNase A in high salt buffer, whereas the slower migrating product was RNase A resistant (Figure 9A, lane 3). Neither product was synthesized using extracts from non-infected tissue, although some fast-migrating, RNase-susceptible products

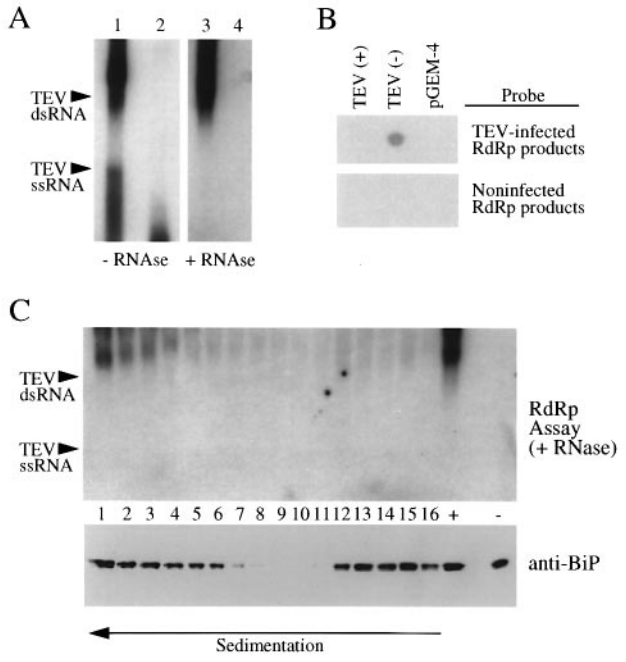

Fig. 9. Analysis of membrane-bound TEV RdRp activity. (**A**) [^{32}P]UTP-labeled RdRp products using P30-2 fractions from TEV-infected (lanes 1 and 3) and non-infected (lanes 2 and 4) plants. Total (lanes 1 and 2) and RNase A-resistant (lanes 3 and 4) products are shown. The markers indicate the electrophoretic positions of synthetic TEV ssRNA and TEV dsRNA. (**B**) Filter hybridization analysis of [^{32}P]UTP-labeled RdRp products using P30-2 fractions from TEV-infected (top) and non-infected (bottom) plants. The RNAs (400 ng) bound to the filter were full-length TEV plus strand RNA, full-length TEV minus strand RNA or RNA transcribed from pGEM-4. (**C**) Analysis of [^{32}P]UTP-labeled RdRp activity and BiP in a sucrose gradient using P30-2 extract from TEV-infected tissue. Each gradient fraction (lanes 1–16), as well as total P30-2 fractions from infected (+) and non-infected (–) plants, was analyzed for RNase A-resistant RdRp activity (top) and subjected to immunoblot analysis using anti-BiP serum (bottom).

were usually, but not always, detected near the agarose gel running front (Figure 9A, lanes 2 and 4). The *in vitro* synthesized products from the infected and non-infected extracts were hybridized to Nytran filter-bound TEV plus strand RNA, TEV minus strand RNA and a non-specific RNA derived from the plasmid pGEM-4. The products synthesized using infected tissue extract hybridized only to TEV minus strand RNA, while products synthesized using the non-infected tissue extract failed to hybridize with any of the RNAs (Figure 9B). These results indicate that the membrane fraction isolated from infected tissue contained an RdRp activity capable of synthesizing TEV plus strand RNA from an endogenous template, and that the plus strand product accumulated in both double-stranded (RNase-resistant) and single-stranded (RNase-susceptible) forms.

The P30-2 fraction from TEV-infected tissue was subjected to sucrose gradient analysis under the 3 mM $MgCl_2$ conditions described above, except that the amount of membrane loaded onto each gradient was ~5-fold greater than in the previous experiments. Gradient fractions were assayed for RdRp activity (RNase A-resistant products) and for the presence of BiP to mark the position of the ER. Most of the RdRp activity was associated with fractions near the bottom of the gradient (Figure 9C). An anomalous electrophoresis pattern, where the RdRp products synthesized in fractions 3–5 migrated more slowly than products synthesized in other fractions, was consistently observed, although this did not interfere with detection of the products. Fractions containing TEV RdRp products also contained BiP (Figure 9C), indicating that the membrane-bound replication complexes co-fractionated with the ER.

Discussion

The interaction between positive strand RNA virus replication complexes and membranes involves crucial events at the virus–cell interface during the infection process. In this study, the TEV 6 kDa protein was shown to be an integral membrane protein that associates specifically, in the presence or absence of other viral factors, with membranes derived from the ER. It was also shown that TEV replication complexes associate with ER-like membranes. The 6 kDa protein is the only known TEV protein that possesses ER localization information. We propose, therefore, that a primary determinant for targeting TEV replication complexes to membranous sites of RNA synthesis involves direct interaction of the 6 kDa protein with the ER.

The large, brightly fluorescing vesicles tagged by GFP/6 represented a subset of ER-like membranes within bombarded or infected cells. The intense fluorescence of relatively few vesicles in each cell could be due to cooperative membrane-binding effects, fusion of many vesicles containing GFP/6 or the presence of relatively few vesicles with competence to interact with GFP/6. Given that the GFP/6-containing membranes exhibited ER-like properties, it is likely that they derived from existing ER. In fact, the organization of the entire cortical ER was found to be altered during TEV infection. The evenly distributed ER network appeared to collapse into loosely connected aggregates upon infection by TEV. The aggregates may actually have been clusters of ER-derived vesicles. Clearly distinct vesicles that were the size of those visualized by GFP/6 fluorescence were not observed in infected cells containing ER-targeted GFP, possibly because the vesicular membranes targeted by GFP/6 were embedded within the ER-derived aggregated structures. Extensive vesiculation is a characteristic cytopathic effect induced by picornavirus supergroup members, including potyviruses (Lesemann, 1988), comoviruses (Eggen and van Kammen, 1988) and picornaviruses (Semler *et al.*, 1988). Vesicle accumulation in comovirus- and picornavirus-infected cells can be induced by expression of a subset of viral proteins required for genome replication (van Bokhoven *et al.*, 1992; Cho *et al.*, 1994: Echeverri and Dasgupta, 1995). Two poliovirus proteins, 2B and 3A, have been shown to inhibit the secretory pathway (Barco and Carrasco, 1995; Doedens and Kirkegaard, 1995), possibly contributing to the build up of vesicles. The induction of vesicle accumulation may be a general mechanism to increase the available surface area for RNA synthesis. The membrane may provide a scaffolding function, as well as provide a mechanism to limit diffusion and increase local concentrations of viral RNA and proteins.

The 6 kDa protein membrane-targeting signal resides

within the central 23 amino acid residues (amino acids 22–44) consisting of the hydrophobic domain and flanking charged residues. This region is both required and sufficient to direct a heterologous protein (GFP) to membranes. The 19 amino acid hydrophobic sequence potentially could span the lipid bilayer once as an α-helix or a random coil, or twice as a two-stranded β-sheet. Alternatively, this region could form a hydrophobic patch that extends partly through the lipid bilayer in a manner proposed for the prostaglandin H_2 synthase-1 (Picot *et al*., 1994). It is speculated that both the N- and C-termini of the 6 kDa protein reside on the cytoplasmic side of the membrane, as this would provide access of NIa proteinase to both cleavage sites.

Regardless of the membrane topology, the 6 kDa protein is probably targeted to the ER-like membrane by an unusual mechanism that differs from the signal recognition particle (SRP)–ER docking pathway. There is no evidence that any region of the polyprotein upstream of the 6 kDa protein sequence is inserted co-translationally into the ER. The 6 kDa protein may belong to a 'non-conformist' class of integral membrane proteins containing C-terminal, or C-terminal-proximal, anchor sequences that insert by a post-translational, SRP-independent pathway (Kutay *et al*., 1993). These tail-anchored proteins, which include cytochrome *b*5 and synaptobrevin, face the cytoplasm with their C-terminal insertion sequence (typically 16–20 amino acids) embedded within the membrane. Some of these proteins, however, are postulated to have insertion sequences that dip in and out of the membrane, resulting in both N- and C-termini on the cytoplasmic face (Kutay *et al*., 1993). The C-terminal hydrophobic sequences (with short flanking regions in some cases) have been shown to be required and sufficient for targeting of synaptobrevin, cytochrome *b*5, microsomal aldehyde dehydrogenase and tyrosine phosphatase PTP 1B to the ER membrane (Frangioni *et al*., 1992; Mitoma and Ito, 1992; Masaki *et al*., 1994; Kutay *et al*., 1995). Interestingly, a 12 residue long hydrophobic sequence consisting mainly of polyleucine was shown to substitute for the C-terminal insertion signal of synaptobrevin in an *in vitro* ER membrane-binding assay (Whitley *et al*., 1996), suggesting that proper targeting and insertion may only require a correctly positioned hydrophobic region with little or no strict sequence requirement. A hydrophobic sequence is a highly conserved feature of the 3A protein encoded by several picornaviruses and may mediate targeting by a similar mechanism (Semler *et al*., 1988). The 3A protein has been postulated to anchor the VPg (3B) to vesicular membranes within the context of a 3AB polyprotein (Semler *et al*., 1982; Takegami *et al*., 1983; Takeda *et al*., 1986; Giachetti and Semler, 1991). Recently, a 22 residue hydrophobic domain within the C-terminal half of the poliovirus 3A protein was shown to be sufficient to mediate an integral association with microsomal membranes *in vitro* (Towner *et al*., 1996). This observation is significant considering the proposed similarity in function of the poliovirus 3A and TEV 6 kDa proteins.

The data presented here are consistent with a model in which TEV replication complexes are anchored to ER-like membranes through a mechanism involving polyproteins containing the 6 kDa protein. Three polyproteins containing the 6 kDa protein sequence have been detected in TEV-infected cells: CI/6, 6/VPg domain and 6/NIa (VPg plus proteinase) (Restrepo-Hartwig and Carrington, 1994). Viral RNA populations contain both full-length NIa and processed VPg domain covalently attached to the 5′ end of individual molecules (Murphy *et al*., 1990a; Carrington *et al*., 1993). Importantly, the membrane-binding activity of the 6 kDa protein overrides the nuclear localization signal of NIa (Restrepo-Hartwig and Carrington, 1992). Direction of VPg or NIa to ER-derived replication sites may involve 6/VPg, 6/NIa or a larger polyprotein that has yet to be detected. If the 6/NIa polyprotein is targeted to membranes, four activities of NIa may then facilitate initiation of RNA synthesis and subsequent release of nascent RNA from the membrane. First, the proteolytic domain of NIa interacts specifically with NIb polymerase (Li *et al*., 1997), which is known to be active in *trans* within infected cells (Li and Carrington, 1995). Second, the NIa proteolytic domain binds RNA (Daròs and Carrington, submitted). The NIb polymerase is postulated to be delivered to the viral RNA template through a NIa proteinase domain–RNA interaction. Third, the VPg domain of NIa serves during initiation of RNA synthesis, possibly as a protein primer as proposed for picornaviruses (Wimmer *et al*., 1993). Fourth, release of NIa from the membrane is facilitated by intramolecular processing at the 6 kDa protein–NIa cleavage site by the NIa proteinase (Carrington and Dougherty, 1987a). While there are a number of differences between initiation models for TEV and poliovirus, a post-translationally inserted membrane-binding protein that anchors a VPg precursor to membranous replication sites may be a universal feature of picornavirus supergroup members.

Materials and methods

Isolation and biochemical treatment of membranes

Leaf tissue from transgenic *Nicotiana tabacum* plants expressing GUS or GUS/6 (Restrepo-Hartwig and Carrington, 1994) was used for the isolation of a crude membrane fraction. 1 g of tissue was ground in 4 ml of buffer Q (50 mM Tris–HCl, pH 7.4, 15 mM $MgCl_2$, 10 mM KCl, 20% glycerol, 0.1% β-mercaptoethanol, 5 μg/ml leupeptin and 2 μg/ml aprotinin), and nuclei, chloroplasts, cell wall and debris were removed by centrifugation at 3000 *g* at 4°C for 10 min. The supernatant was subjected to centrifugation at 30 000 *g* at 4°C for 30 min, resulting in soluble (S30) and crude membrane (P30) fractions. For alkaline extraction, the P30 pellet was resuspended in 0.1 M Na_2CO_3, pH 10.5, 4 mM EDTA and 4 mM phenylmethylsulfonyl fluoride (PMSF). For urea extraction, the P30 pellet was resuspended in 25 mM HEPES, pH 6.8, 4 mM EDTA, 4 mM PMSF and 4 M urea. For salt extraction, the P30 pellet was resuspended in buffer Q containing 1 M KCl. In each extraction, the samples were incubated on ice for 30 min, then subjected to centrifugation at 30 000 *g* at 4°C for 30 min. The pellets were resuspended in protein dissociation buffer in volumes equal to those of the corresponding supernatants. Equivalent amounts of samples were analyzed by immunoblot analysis with anti-GUS serum (obtained from Tom McKnight, Texas A & M University) after electrophoresis through 12.5% polyacrylamide gels.

Triton X-114 phase partitioning was done according to Bordier (1981) using P30 fractions obtained from GUS/6 transgenic leaf tissue. The final aqueous and detergent-soluble phases were equalized according to volume using protein dissociation buffer and subjected to immunoblot analysis using anti-GUS serum.

Transient expression of GFP/6 fusion proteins

The plasmid pRTL2-mGFP was constructed by subcloning the GFP-coding sequence between codon 186 and the 3′ end from pBIN35S-mGFP4 (obtained from Jim Haseloff, MRC Laboratory) into pRTL2-GFP (obtained from Albrecht von Arnim, University of Tennessee). pRTL2-GFP contains a *Bgl*II site (AGATCT) introduced

after the last GFP codon but before the stop codon. The 6 kDa protein-coding sequence was amplified by PCR from pTEV7DA using primers that included a *Bgl*II site at each end. The resulting product was subcloned into the *Bgl*II site of pRTL2-mGFP. The base vector for these constructs, pRTL2 (Carrington *et al*., 1990), contains an enhanced cauliflower mosaic virus 35S promoter, TEV 5′-non-translated region and the 35S termination sequence to facilitate expression in plant cells.

Sequences were deleted from the 6 kDa protein-coding region in pRTL2-mGFP/6 using an inverse PCR method. Sets of primers that annealed to sequences adjacent to the 5′ and 3′ deletion borders within the 6 kDa protein-coding region, and that initiated DNA synthesis away from the deleted sequences, were used in PCR with pRTL2-mGFP/6 as the template. The 5′ end of each primer contained a *Kpn*I restriction site. The linear PCR product was digested with *Kpn*I, self-ligated and used to transform *Escherichia coli* strain DH5α. Five deletion mutants that lacked the following sequences were generated: codons 1–21 (GFP/6Δ1–21); codons 45–52 (GFP/6Δ45–52); codons 24–42 (GFP/6Δ24–42); codons 24–32 (GFP/6Δ24–32); and codons 33–42 (GFP/6Δ33–42). The modified sequence coding for the truncated 6 kDa proteins was determined in each construct to verify that no inadvertent changes were introduced.

A series of three double deletion mutants were generated using a similar inverse PCR strategy, but with plasmid templates containing one of the deletions described above. The double deletion mutants lacked the following 6 kDa protein coding sequences: codons 1–21 and 45–52 (GFP/6.22–44); codons 1–32 and 45–52 (GFP/6.33–44); and codons 1–21 and 33–52 (GFP/6.22–32).

The pRTL2-mGFP- and pRTL2-mGFP/6-derived plasmids were used for biolistic transfection of tobacco epidermal cells using a helium-driven microprojectile bombardment system (PDS-1000/He system, Biorad Laboratories). Plasmid DNA (1 μg) was precipitated onto 1.6 μm gold particles (0.5 mg) in the presence of 1 M $CaCl_2$, 6.25 mM spermidine, and washed with 35% ethanol. Tobacco leaves were excised and bombarded with the DNA-coated gold particles at 500–900 p.s.i. and incubated in water for 12–20 h under fluorescent light at room temperature. Leaf pieces were cut into small squares (~0.5 cm^2), vacuum-infiltrated with water to remove air spaces between cells, and placed on microscope slides under a coverslip. The samples were viewed by brightfield and fluorescence microscopy using an Olympus BX50 microscope with the DM 500 dichroic mirror/BP470–490 exciter filter/BA515 barrier filter set. Photomicrographs were taken with Kodak Ektachrome 100 daylight film.

Recombinant TEV expressing GFP or GFP/6

The GFP and GFP/6 sequences were introduced into a full-length TEV cDNA-containing plasmid, pTEV7DA-CMK, which contains a polylinker consisting of *Nco*I, *Cla*I, *Mlu*I and *Kpn*I between the P1- and HC-Pro-coding sequences. The modified TEV sequence in pTEV7DA-CMK also contains the sequences coding for a NIa proteinase recognition site between the *Kpn*I site and the 5′ end of the HC-Pro sequence. The GFP and GFP/6 sequences were amplified by PCR such that the 5′ and 3′ ends contained *Cla*I and *Kpn*I sites, respectively. The PCR products were digested with *Cla*I and *Kpn*I and inserted between the *Cla*I and *Kpn*I sites of pTEV7DA-CMK, resulting in pTEV7DA-GFP and pTEV7DA-GFP/6. Infectious RNA transcripts were generated by linearization of pTEV7DA-GFP and pTEV7DA-GFP/6 with *Bgl*II and transcription in the presence of m^7GpppG cap analog with SP6 RNA polymerase (Ambion, Inc.) as described (Dolja *et al*., 1992). Concentrated transcripts were used to inoculate tobacco plants, and virus stocks (TEV-GFP and TEV-GFP/6) were prepared at 5 days post-inoculation (d p.i.).

To view GFP or GFP/6 fluorescence expressed using engineered TEV vectors, protoplasts were prepared from non-infected plants and from TEV-GFP- or TEV-GFP/6-infected plants (two or three leaves above the top inoculated leaf) at 5 d p.i. Protoplasts were analyzed using brightfield and fluorescence photomicroscopy as described above. The resulting slides were scanned and digitized using a Nikon LS-1000 Film Scanner and Adobe Photoshop 3.0 software (Adobe Systems Incorporated). The images were modified digitally by subtraction of red color that resulted from autofluorescence of chloroplasts.

Immunofluorescence microscopy

Tobacco plants were inoculated with TEV-GFP or TEV-GFP/6 and protoplasts were isolated from systemically infected leaf tissue at 5 d p.i. Protoplasts (5×10^5) were fixed in phosphate-buffered saline (PBS; 140 mM NaCl, 2.5 mM KCl, 10 mM Na_2HPO_4, 1.5 mM KH_2PO_4) containing 4% paraformaldehyde (EMS) for 1 h at room temperature and collected by centrifugation at 80 *g*. Protoplasts were incubated in two changes of 95% ethanol, each for 5 min, at room temperature, and then rehydrated through a series of ethanol/PBS washes starting with 75% ethanol, followed by 50, 25 and 0% ethanol steps. Protoplasts were incubated overnight at 4°C in blocking buffer (PBS, 5% dry milk and 5% sheep serum). Polyclonal rabbit anti-BiP and anti-β-xylosyl sera (both obtained from Maarten Chrispeels, University of California, San Diego) were diluted 1:1000 and 1:10 000, respectively, in blocking buffer and incubated with protoplasts for 30 min at room temperature on a rotator. Protoplasts were then washed five times for 10 min each in PBS/Tween [PBS, 0.1% bovine serum albumin (BSA), 0.05% sodium azide, pH 7.2, and 0.05% Tween-20]. The secondary antibody, Cy3-conjugated sheep anti-rabbit IgG at 1:500 dilution in blocking buffer, was incubated with the protoplasts for 30 min at room temperature on a rotator. Protoplasts were washed five times for 10 min each in PBS/Tween, resuspended in SlowFade-Light/Equilibration buffer (Molecular Probes, Inc.) in 50% glycerol and mounted on glass microscope slides with a coverslip.

Fluorescence microscopy was conducted using two filter sets for each field of view. For GFP fluorescence, the DM 500 dichroic mirror/BP470–490 exciter filter/BA515 barrier filter set was used. For Cy3 fluorescence, the DM 570 dichroic mirror/BP530–550 exciter filter/BA590 barrier filter set was used. Photomicrographs were taken with Kodak Ektachrome 100 film. Co-localization of GFP/6 with BiP or β-xylosyl was assessed by scoring 64 or 87 random protoplasts, respectively. The percentage of cells that contained strong, weak or no co-localization of GFP and Cy3 fluorescence was recorded.

Transgenic plants expressing ER-targeted GFP

Transgenic *N.benthamiana* plants expressing an ER-targeted form of GFP (mGFP5, from Dr Jim Haseloff) were supplied by Dr David Baulcombe (Sainsbury Laboratory). Plants were inoculated with TEV (HATr strain). Strips of epidermal cells were peeled from the underside of systemically infected leaves within 48 h of symptom appearance, mounted in water under coverslips and viewed by fluorescence microscopy to detect GFP.

Membrane fractionation

Leaf tissue (2 g) from plants systemically infected by TEV-GFP or TEV-GFP/6 was minced for 10 min in 6 ml of homogenization buffer [50 mM Tris–HCl, pH 8.0, 10 mM KCl, 0.1 mM or 3 mM $MgCl_2$, 1 mM EDTA, 1 mM dithiothreitol (DTT), 0.1% BSA, 0.3% dextran, 13% sucrose, 5 μg/ml leupeptin and 2 μg/ml aprotinin] (Gardiner and Chrispeels, 1975; Wienecke *et al*., 1982). The homogenate was filtered through Miracloth and subjected to centrifugation at 3700 *g* for 10 min at 4°C. A portion of the supernatant (S3, 2.5 ml) was layered onto a 9 ml 20–45% sucrose gradient containing the respective homogenization buffer and subjected to centrifugation at 143 000 *g* in a Beckman SW41 Ti rotor for 4 h at 4°C. Fractions (0.7 ml) were collected from the bottom of each gradient after tube puncture. The fractions were diluted 1:1 in protein dissociation buffer and subjected to immunoblot analysis after 12.5% polyacrylamide gel electrophoresis. Four polyclonal antisera were used: anti-BiP and anti-β-xylosyl sera (described above), anti-protein disulfide isomerase serum (from Richard Dixon, Samuel Roberts Noble Foundation) and anti-GFP (Clontech Laboratories). Immunoreactions were detected using a chemiluminescence-based secondary antibody system (Amersham, Inc.).

RNA-dependent RNA polymerase assays

Leaf tissue (10 g) from plants systemically infected by TEV (HATr strain) or non-infected plants was minced in 30 ml of homogenization buffer (with 3 mM $MgCl_2$), and an S3 fraction was prepared as described above. The S3 fraction was subjected to centrifugation at 30 000 *g* for 20 min at 4°C, and the P30 fraction was reconstituted in homogenization buffer with the aid of a Dounce homogenizer and subjected to centrifugation again at 30 000 *g* for 20 min at 4°C (P30-2). The P30-2 pellet was resuspended in 2.6 ml of homogenization buffer, and 2.5 ml was layered onto a 20–45% sucrose gradient containing homogenization buffer. The gradients were processed as described above. RdRp assays were done for 1 h at 28°C in reactions containing 50 μl of gradient fraction or resuspended P30-2 fraction, 50 mM Tris, pH 8.2, 10 mM $MgCl_2$, 10 mM DTT, 1 mM ATP, 1 mM CTP, 1 mM GTP, 10 μM UTP and 10 μCi of [α-^{32}P]UTP (800 μCi/mmol) (Quadt *et al*., 1991). After addition of SDS (2%), the reaction products were digested at 37°C for 15 min with proteinase K (1.4 mg/ml, Gibco-BRL), extracted using phenol–chloroform and precipitated in ethanol. The products were resuspended in 60 μl of deionized H_2O, and 10 μl of sample was digested with RNase A (1.25 μg/ml, Sigma) in the presence of 233 mM NaCl, 3.3 mM Tris–

HCl, pH 7.4, 10 mM EDTA, at 30°C for 15 min (Sawicki and Sawicki, 1990). The RNase A-treated products were then reacted with proteinase K (5 mg/ml) in the presence of 2% SDS at 37°C for 30 min. RNase A-treated and non-treated RdRp products were analyzed by electrophoresis through 1% agarose gels, followed by autoradiography.

Dot-blot hybridization was done using RdRp products from reactions containing P30-2 fractions from infected and non-infected plants as probes. Duplicate Nytran filters (Schleicher and Schuell) contained 400 ng of each of three RNA transcripts: full-length TEV plus strand RNA, full-length TEV minus strand RNA and pGEM4-derived RNA. The TEV plus and minus strand RNAs were synthesized by transcription of pTEV7DA using SP6 and T7 RNA polymerases, respectively. The RNAs were fixed to the filters by UV irradiation and hybridized with heat-denatured RdRp products at 65°C for 6 h in a hybridization incubator (Robbins Scientific) using standard methods. The filters were washed in four changes of 2× SSC, 0.02% SDS, and in four changes of 0.2× SSC, 0.1% SDS at 75°C, after which they were dried and exposed to Kodak BIOMAX MS film with an intensifying screen at –90°C.

Acknowledgements

We thank Albrecht von Arnim and Jim Haseloff for the modified GFP plasmids, David Baulcombe for transgenic plants expressing ER-targeted GFP, Tom McKnight for anti-GUS serum, Maarten Chrispeels for anti-BiP and anti-β-xylosyl sera, and Rick Dixon for anti-PDI serum. We also thank Ruth Haldeman-Cahill for construction of several plasmids, Larry Griffing for assistance with immunofluorescence microscopy and subcellular fractionation, Mike Plamann for the use of his slide scanner and José-Antonio Daròs for many helpful discussions. This research was supported by a grant (AI27832 to J.C.C.) and NRSA Fellowship (AI09121 to M.C.S.) from the National Institutes of Health.

References

Allison,R., Johnston,R.E. and Dougherty,W.G. (1986) The nucleotide sequence of the coding region of tobacco etch virus genomic RNA: evidence for the synthesis of a single polyprotein. *Virology*, **154**, 9–20.

Barco,A. and Carrasco,L. (1995) A human virus protein, poliovirus protein 2BC, induces membrane proliferation and blocks the exocytic pathway in the yeast *Saccharomyces cerevisiae*. *EMBO J.*, **14**, 3349–3346.

Baunoch,D., Das,P. and Hari,V. (1988) Intracellular localization of TEV capsid and inclusion proteins by immunogold labeling. *J. Ultrastruct. Mol. Struct. Res.*, **99**, 203–212.

Bienz,K., Egger,D., Rasser,Y. and Bossart,W. (1983) Intracellular distribution of poliovirus proteins and the induction of virus-specific cytoplasmic structures. *Virology*, **131**, 39–48.

Bienz,K., Egger,D. and Pasamontes,L. (1987) Association of polioviral proteins of the P2 genomic region with the viral replication complex and virus-induced membrane synthesis as visualized by electron microscopic immunocytochemistry and autoradiography. *Virology*, **160**, 220–226.

Bienz,K., Egger,D., Pfister,T. and Troxler,M. (1992) Structural and functional characterization of the poliovirus replication complex. *J. Virol.*, **66**, 2740–2747.

Boevink,P., Santa Cruz,S., Hawes,C., Harris,N. and Oparka,K.J. (1996) Virus-mediated delivery of the green fluorescent protein to the endoplasmic reticulum of plant cells. *Plant J.*, **10**, 935–941.

Bordier,C. (1981) Phase separation of integral membrane proteins in Triton X-114 solution. *J. Biol. Chem.*, **256**, 1604–1607.

Carrington,J.C. and Dougherty,W.G. (1987a) Processing of the tobacco etch virus 49K protease requires autoproteolysis. *Virology*, **160**, 355–362.

Carrington,J.C. and Dougherty,W.G. (1987b) Small nuclear inclusion protein encoded by a plant potyvirus genome is a protease. *J. Virol.*, **61**, 2540–2548.

Carrington,J.C., Freed,D.D. and Oh,C.-S. (1990) Expression of potyviral polyproteins in transgenic plants reveals three proteolytic activities required for complete processing. *EMBO J.*, **9**, 1347–1353.

Carrington,J.C., Haldeman,R., Dolja,V.V. and Restrepo-Hartwig,M.A. (1993) Internal cleavage and *trans*-proteolytic activities of the VPg-proteinase (NIa) of tobacco etch potyvirus *in vivo*. *J. Virol.*, **67**, 6995–7000.

Chalfie,M., Tu,Y., Euskirchen,G., Ward,W.W. and Prasher,D.C. (1994) Green fluorescent protein as a marker for gene expression. *Science*, **263**, 802–805.

Cho,M.W., Teterina,N., Egger,D., Bienz,K. and Ehrenfeld,E. (1994) Membrane rearrangement and vesicle induction by recombinant poliovirus 2C and 2BC in human cells. *Virology*, **202**, 129–145.

Doedens,J.R. and Kirkegaard,K. (1995) Inhibition of cellular protein secretion by poliovirus proteins 2B and 3A. *EMBO J.*, **14**, 894–907.

Dolja,V.V., McBride,H.J. and Carrington,J.C. (1992) Tagging of plant potyvirus replication and movement by insertion of β-glucuronidase into the viral polyprotein. *Proc. Natl Acad. Sci. USA*, **89**, 10208–10212.

Dolja,V.V., Haldeman,R., Robertson,N.L., Dougherty,W.G. and Carrington,J.C. (1994) Distinct functions of capsid protein in assembly and movement of tobacco etch potyvirus in plants. *EMBO J.*, **13**, 1482–1491.

Domier,L.L., Shaw,J.G. and Rhoads,R.E. (1987) Potyviral proteins share amino acid sequence homology with picorna-, como-, and caulimoviral proteins. *Virology*, **158**, 20–27.

Dougherty,W.G. and Semler,B.L. (1993) Expression of virus-encoded proteinases: functional and structural similarities with cellular enzymes. *Microbiol. Rev.*, **57**, 781–822.

Echeverri,A.C. and Dasgupta,A. (1995) Amino terminal regions of poliovirus 2C protein mediate membrane binding. *Virology*, **208**, 540–553.

Eggen,R. and van Kammen,A. (1988) RNA replication in Comoviruses. In Ahlquist,P., Holland,J. and Domingo,E. (eds), *RNA Genetics*. CRC Press, Boca Raton, FL, Vol. I, pp. 49–69.

Frangioni,J.V., Beahm,P.H., Shifrin,V., Jost,C.A. and Neel,B.G. (1992) The nontransmembrane tyrosine phosphatase PTP 1B localizes to the endoplasmic reticulum via its 35 amino acid C-terminal sequence. *Cell*, **68**, 545–560.

García,J.A., Riechmann,J.L. and Laín,S. (1989) Proteolytic activity of the plum pox potyvirus NIa-like protein in *Escherichia coli*. *Virology*, **170**, 362–369.

Gardiner,M. and Chrispeels,M.J. (1975) Involvement of the Golgi apparatus in the synthesis and secretion of hydroxyproline-rich cell wall glycoprotein. *Plant Physiol.*, **55**, 536–541.

Giachetti,C. and Semler,B.L. (1991) Role of a viral membrane polypeptide in strand-specific initiation of poliovirus RNA synthesis. *J. Virol.*, **65**, 2647–2654.

Hellmann,G.M., Shaw,J.G. and Rhoads,R.E. (1988) *In vitro* analysis of tobacco vein mottling virus NIa cistron: evidence for a virus-encoded protease. *Virology*, **163**, 554–562.

Hong,Y., Levay,K., Murphy,J.F., Klein,P.G., Shaw,J.G. and Hunt,A.G. (1995) The potyvirus polymerase interacts with the viral coat protein and VPg in yeast cells. *Virology*, **214**, 159–166.

Klein,PG., Klein,RR., Rodríguez-Cerezo,E., Hunt,A.G. and Shaw,J.G. (1994) Mutational analysis of the tobacco vein mottling virus genome. *Virology*, **204**, 759–769.

Koonin,E.V. and Dolja,V.V. (1993) Evolution and taxonomy of positive-strand RNA viruses: implications of comparative analysis of amino acid sequences. *Crit. Rev. Biochem. Mol. Biol.*, **28**, 375–430.

Kutay,U., Hartmann,E. and Rapoport,T.A. (1993) A class of membrane proteins with a C-terminal anchor. *Trends Cell Biol.*, **3**, 72–75.

Kutay,U., Ahnert-Hilger,G., Hartmann,E., Wiedenmann,B. and Rapoport,T.A. (1995) Transport route for synaptobrevin via a novel pathway of insertion into the endoplasmic reticulum membrane. *EMBO J.*, **14**, 217–223.

Laín,S., Riechmann,J.L. and García,J.A. (1990) RNA helicase: a novel activity associated with a protein encoded by a positive-strand RNA virus. *Nucleic Acids Res.*, **18**, 7003–7006.

Laín,S., Martín,M.T., Riechmann,J.L. and García,J.A. (1991) Novel catalytic activity associated with positive-strand RNA virus infection: nucleic acid-stimulated ATPase activity of the plum pox potyvirus helicase protein. *J. Virol.*, **65**, 1–6.

Laurière,M., Laurière,C., Chrispeels,M.J., Johnson,K.D. and Sturm,A. (1989) Characterization of a xylose-specific antiserum that reacts with the complex asparagine-linked glycans of the extracellular and vacuolar glycoproteins. *Plant Physiol.*, **90**, 1182–1188.

Lesemann,D.-E. (1988) Cytopathology. In Milne,R.G. (ed.), *The Plant Viruses—The Filamentous Plant Viruses*. Plenum Publishing Corporation, New York, Vol. 4, pp. 179–235.

Li,X.H. and Carrington,J.C. (1995) Complementation of tobacco etch potyvirus mutants by active RNA polymerase expressed in transgenic cells. *Proc. Natl Acad. Sci. USA*, **92**, 457–461.

Li,X.H., Valdez,P., Olvera,R.E. and Carrington,J.C. (1997) Functions of the tobacco etch virus RNA polymerase (NIb): subcellular transport and protein–protein interaction with VPg/proteinase (NIa) *J. Virol.*, **71**, 1598–1607.

Lord,J.M., Kagawa,T., Moore,T.S. and Beevers,H. (1973) Endoplasmic reticulum as the site of lecithin formation in castor bean endosperm. *J. Cell Biol.*, **57**, 659–667.

Masaki,R., Yamamoto,A. and Tashiro,Y. (1994) Microsomal aldehyde dehydrogenase is localized to the endoplasmic reticulum via its carboxy-terminal 35 amino acids. *J. Cell Biol.*, **126**, 1407–1420.

Mitoma,J. and Ito,A. (1992) The carboxy-terminal 10 amino acid residues of cytochrome b_5 are necessary for its targeting to the endoplasmic reticulum. *EMBO J.*, **11**, 4197–4203.

Murphy,J.F., Rhoads,R.E., Hunt,A.G. and Shaw,J.G. (1990a) The VPg of tobacco etch virus RNA is the 49 kDa proteinase or the N-terminal 24 kDa part of the proteinase. *Virology*, **178**, 285–288.

Murphy,J.F., Rychlik,W., Rhoads,R.E., Hunt,A.G. and Shaw,J.G. (1990b) A tyrosine residue in the small nuclear inclusion protein of tobacco vein mottling virus links the VPg to the viral RNA. *J. Virol.*, **65**, 511–513.

Murphy,J.F., Klein,P.G., Hunt,A.G. and Shaw,J.G. (1996) Replacement of the tyrosine residue that links a potyviral VPg to the viral RNA is lethal. *Virology*, **220**, 535–538.

Picot,D., Loll,P.J. and Garavito,R.M. (1994) The X-ray crystal structure of the membrane protein prostaglandin H_2 synthase-1. *Nature*, **367**, 243–249.

Quadt,R., Rosdorff,H.J.M., Hunt,T.W. and Jaspers,E.M.J. (1991) Analysis of the protein composition of alfalfa mosaic virus RNA-dependent RNA polymerase. *Virology*, **182**, 309–315.

Restrepo,M.A., Freed,D.D. and Carrington,J.C. (1990) Nuclear transport of plant potyviral proteins. *Plant Cell*, **2**, 987–998.

Restrepo-Hartwig,M.A. and Carrington,J.C. (1992) Regulation of nuclear transport of a plant potyvirus protein by autoproteolysis. *J. Virol.*, **66**, 5662–5666.

Restrepo-Hartwig,M.A. and Carrington,J.C. (1994) The tobacco etch potyvirus 6-kilodalton protein is membrane-associated and involved in viral replication. *J. Virol.*, **68**, 2388–2397.

Sawicki,S.G. and Sawicki,D.L. (1990) Coronavirus transcription: subgenomic mouse hepatitis virus replicative intermediates function in RNA synthesis. *J. Virol.*, **64**, 1050–1056.

Schaad,M.C., Haldeman-Cahill,R., Cronin,S. and Carrington,J.C. (1996) Analysis of the VPg-proteinase (NIa) encoded by tobacco etch potyvirus: effects of mutations on subcellular transport, proteolytic processing and genome amplification. *J. Virol.*, **70**, 7039–7048.

Semler,B.L., Anderson,C.W., Hanecak,R., Dorner,L.F. and Wimmer,E. (1982) A membrane-associated precursor to poliovirus VPg identified by immunoprecipitation with antibodies directed against a synthetic heptapeptide. *Cell*, **28**, 405–412.

Semler,B.L., Kuhn,R.J. and Wimmer,E. (1988) Replication of the poliovirus genome. In Ahlquist,P., Holland,J. and Domingo,E. (eds), *RNA Genetics*. CRC Press, Inc., Boca Raton, FL, Vol. 1, pp. 23–48.

Shahabuddin,M., Shaw,J.G. and Rhoads,R.E. (1988) Mapping of the tobacco vein mottling virus VPg cistron. *Virology*, **163**, 635–637.

Strauss,J.H. and Strauss,E.G. (1994) The aphaviruses: gene expression, replication, and evolution. *Microbiol. Rev.*, **58**, 491–562.

Takeda,N., Kuhn,R.J., Yang,C.F., Takegami,T. and Wimmer,E. (1986) Initiation of poliovirus plus-strand RNA synthesis in a membrane complex of infected HeLa cells. *J. Virol.*, **60**, 43–53.

Takegami,T., Semler,B.L., Anderson,C.W. and Wimmer,E. (1983) Membrane fractions active in poliovirus RNA replication contain VPg precursor polypeptides. *Virology*, **128**, 33–47.

Towner,J.S., Ho,T.V. and Semler,B.L. (1996) Determinants of membrane association for poliovirus protein 3AB. *J. Biol. Chem.*, **271**, 26810–26818.

Troxler,M., Egger,D., Pfister,T. and Bienz,K. (1992) Intracellular localization of poliovirus RNA by *in situ* hybridization at the ultrastructural level using single-stranded riboprobes. *Virology*, **191**, 687–697.

van Bokhoven,H., van Lent,J.W.M., Custers,R., Vlak,J.M., Wellink,J. and van Kammen,A. (1992) Synthesis of the complete 200K polyprotein encoded by cowpea mosaic virus B-RNA in insect cells. *J. Gen. Virol.*, **73**, 2775–2784.

Whitley,P., Grahn,E., Kutay,U., Rapoport,T.A. and von Heijne,G. (1996) A 12-residue long polyleucine tail is sufficient to anchor synaptobrevin to the endoplasmic reticulum membrane. *J. Biol. Chem.*, **271**, 7583–7586.

Wienecke,K., Glas,R. and Robinson,D.G. (1982) Organelles involved in the synthesis and transport of hydroxyproline-containing glycoproteins in carrot root disks. *Planta*, **155**, 58–63.

Wimmer,E., Hellen,C.U. and Cao,X. (1993) Genetics of poliovirus. *Annu. Rev. Genet.*, **27**, 353–436.

Zhang,G.F. and Staehlin,L.A. (1992) Functional compartmentation of the Golgi apparatus of plant cells. *Plant Physiol.*, **99**, 1070–1083.

Received on October 30, 1996; revised on March 21, 1997